

Stratigraphic constraints on late Pleistocene glacial erosion and deglaciation of the Chukchi margin, Arctic Ocean

Leonid Polyak^{a,*}, Dennis A. Darby^b, Jens F. Bischof^b, Martin Jakobsson^c

^a Byrd Polar Research Center, Ohio State University, Columbus, OH 43210, USA

^b Department of Ocean, Earth, and Atmospheric Sciences, Old Dominion University, Norfolk, VA 23529, USA

^c Department of Geology and Geochemistry, Stockholm University, Stockholm, Sweden

Received 9 August 2005

Available online 29 January 2007

Abstract

At least two episodes of glacial erosion of the Chukchi margin at water depths to ~450 m and 750 m have been indicated by geophysical seafloor data. We examine sediment stratigraphy in these areas to verify the inferred erosion and to understand its nature and timing. Our data within the eroded areas show the presence of glaciogenic diamictos composed mostly of reworked local bedrock. The diamictos are estimated to form during the last glacial maximum (LGM) and an earlier glacial event, possibly between OIS 4 to 5d. Both erosional events were presumably caused by the grounding of ice shelves originating from the Laurentide ice sheet. Broader glaciological settings differed between these events as indicated by different orientations of flutes on eroded seafloor. Postglacial sedimentation evolved from iceberg-dominated environments to those controlled by sea-ice rafting and marine processes in the Holocene. A prominent minimum in planktonic foraminiferal $\delta^{18}\text{O}$ is identified in deglacial sediments at an estimated age near 13,000 cal yr BP. This $\delta^{18}\text{O}$ minimum, also reported elsewhere in the Amerasia Basin, is probably related to a major Laurentide meltwater pulse at the Younger Dryas onset. The Bering Strait opening is also marked in the composition of late deglacial Chukchi sediments.

© 2006 University of Washington. All rights reserved.

Keywords: Chukchi margin; Arctic Ocean; Late Pleistocene; Last glacial maximum; Last deglaciation; Holocene; Sediment stratigraphy; Ice grounding; Glaciomarine sedimentation; Meltwater event

Introduction

New high-resolution geophysical mapping of relatively elevated seafloor areas in the Arctic Ocean such as the Lomonosov Ridge, Chukchi Borderland, and Yermak Plateau provide evidence for widespread glaciogenic erosion, shedding light on the dramatic history of the Arctic Ocean during glacial times (Fig. 1A; Vogt et al., 1994; Jakobsson, 1999; Polyak et al., 2001; Kristoffersen et al., 2004; Jakobsson et al., 2005). A striking example is the crest of the Lomonosov Ridge that is truncated to water depths of almost 1000 m along a stretch of ~60 km at the very center of the Arctic Ocean, with the eroded sediment dumped on one side of the ridge. Seismostratigraphy of the eroded area is characterized

by a prominent unconformity overlain by a veneer of unstratified sediment with hard acoustic impedance and multiple parallel, low-relief lineations (flutes) at the surface, similar to numerous examples from formerly glaciated continental margins (e.g., Davies et al., 1997; Shipp et al., 1999; Ó Cofaigh et al., 2003). Although there are two interpretations of the exact agents of this erosion on the Lomonosov Ridge, by ice shelf or armada of closed-up megabergs (Polyak et al., 2001; Jakobsson et al., 2001; Kristoffersen et al., 2004), they both imply glaciogenic origin. Similar erosional features are found over a much larger area on the Chukchi Borderland, which extends into the interior of the Amerasia Basin (Fig. 1A) (Polyak et al., 2001; Jakobsson et al., 2005). These features include sets of lineations reaching tens of kilometers in length, sometimes in combination with a system of nested transverse ridges (Polyak et al., 2001), which unambiguously indicate the

* Corresponding author. Fax: +1 614 292 4697.

E-mail address: polyak.1@osu.edu (L. Polyak).

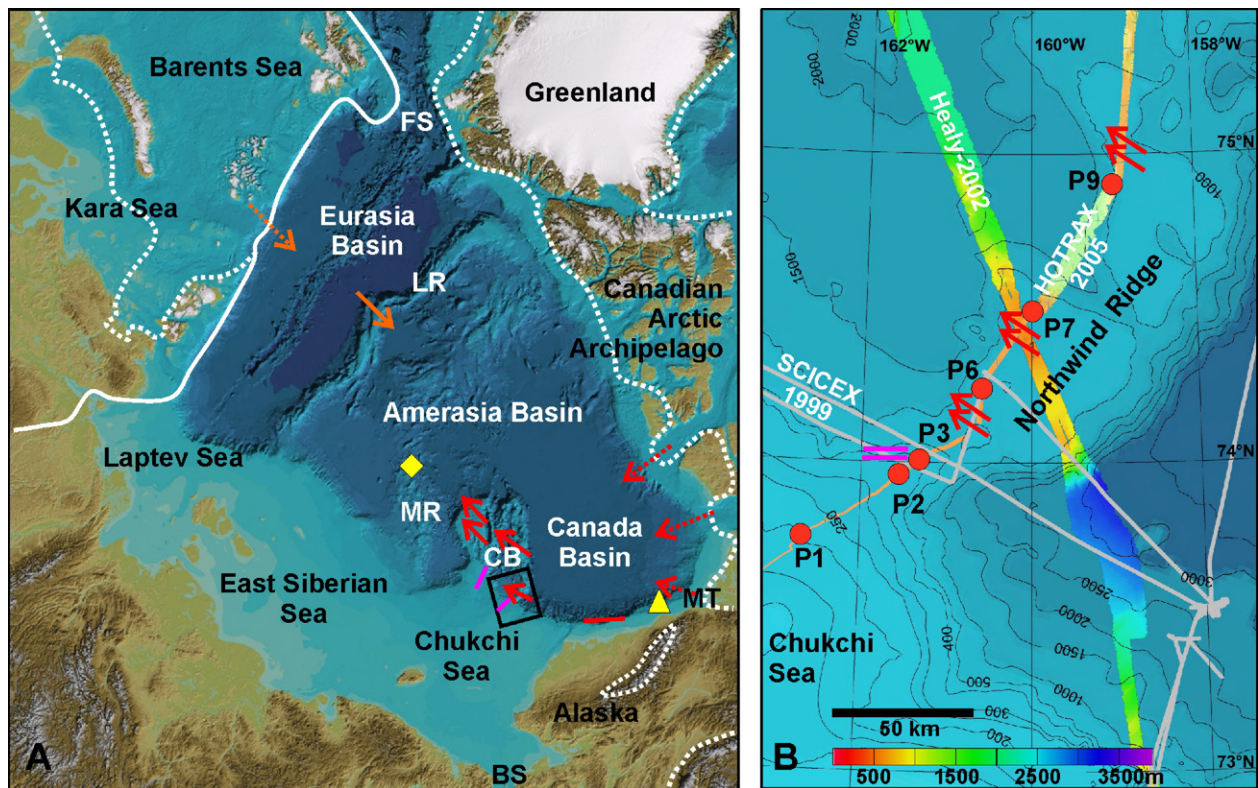


Figure 1. (A) Bathymetric map of the Arctic Ocean (IBCAO) with mapped glaciogenic directional features (solid bars/arrows) and suggested provenance (dotted arrows) (after Polyak et al., 2001; Engels, 2004). Arrowheads show direction of ice flow, where identified. Study area is boxed. Yellow diamond and triangle show location of cores 94-B17 (Poore et al., 1999) and P45 (Andrews and Dunhill, 2004), respectively. LR—Lomonosov Ridge, MR—Mendelev Ridge, CB—Chukchi Borderland, MT—Mackenzie Trough, FS—Fram Strait, BS—Bering Strait. Ice-sheet limits are outlined in white: dashed—LGM, solid—Eurasian OIS 6 (Dyke et al., 2002; Svendsen et al., 2004). (B) Study area (ramp to Northwind Ridge) with location of P1-92-AR sediment cores and geophysical survey lines: light gray—SCICEX-1999, colored multibeam—Healy-2002 and 2005 (HOTRAX) data. Magenta and red bars/arrows near core sites show orientation of fluted fields 1 and 2, respectively (Polyak et al., 2001; Jakobsson et al., 2005).

grounding of a large, cohesive ice mass. At water depths shallower than those of the fluted fields, the seafloor is excavated with abundant, wavy, typically chaotic plowmarks that obliterate pre-existing bedforms.

Sediment cores from the eroded portion of the Lomonosov Ridge confirm the presence of a hiatus beneath a thin layer of recent sediments (Jakobsson et al., 2001). Their stratigraphy indicates that the last erosional event at this site probably occurred during Oxygen Isotope Stage (OIS) 6, ca. 150,000 yr ago. This age of erosion matches the reconstruction of a huge ice sheet in northern Eurasia during OIS 6 based on compelling glacial–geological evidence (Svendsen et al., 2004). The stratigraphy of glaciogenic features on the Chukchi Borderland is much less understood than on the Lomonosov Ridge, which severely restricts our ability to reconstruct the glacial history of the Arctic Ocean. The synchronicity of ice-shelf advances on the American and Eurasian sides of the ocean, if established, may lend credence to the existence of the much-argued pan-Arctic ice sheet (Mercer, 1970; Hughes et al., 1977; Grosswald and Hughes, 1999). Alternatively, asynchronous ice shelves or iceberg armadas would argue for a more complex pattern involving partial and variable coverage of the ocean by deep-draft ice during different glacial periods. Of particular

interest is the configuration of grounded and floating ice sheets during the last glacial maximum (LGM) that is used as a reference time slice in many paleoclimatic models (e.g., Budd et al., 1998; Siegert and Marsiat, 2001; Bromwich et al., 2004).

In the Amerasia Basin, several lines of evidence indicate that extensive ice masses repeatedly covered the basin during glacial periods. This evidence includes: (1) sedimentary records showing abiotic intervals with very low sedimentation or even hiatuses (Poore et al., 1999; Polyak et al., 2004), (2) geomorphic imprints of very large paleo-ice streams funneling through the inter-island channels of the Canadian Arctic Archipelago and the Mackenzie Trough (Blasco et al., 1990; Stokes et al., 2005, 2006), and (3) ice-grounding and erosional bedforms on the Chukchi Borderland and adjacent Alaska/Beaufort margin (Polyak et al., 2001; Engels, 2004; Jakobsson et al., 2005). At least two generations of flutes with differing direction occur on the Chukchi Borderland at different water depths, thus indicating multiple erosional events (Polyak et al., 2001). Here we will explore the sedimentary stratigraphy in the eroded areas to verify the asynchronicity of these events and to estimate their ages. We will primarily focus on the younger event to test its relationship to the LGM.

Glaciogenic bedforms on the Chukchi Borderland

The Chukchi Borderland is a complex of geologic structures rising to relatively shallow water depths (<1000 m) that extends into the Amerasia Basin from the Chukchi shelf and includes the Chukchi Plateau (Cap) and Rise and the Northwind Ridge (Fig. 1A). Original echo-soundings of the Chukchi Plateau registered an abnormally rough seafloor at depths to 300–400 m, interpreted as iceberg scouring (Hunkins et al., 1962; Phillips and Grantz, 1997). Recent seafloor surveys with a 12-kHz swath bathymetry and sidescan and penetration sonar confirmed the abundance of randomly oriented scours, but they also disclosed numerous and diverse bedforms indicative of large-scale erosion and sculpting of the seafloor to water depths approaching 1000 m (Polyak et al., 2001; Jakobsson et al., 2005; Darby et al., 2005). Chaotic, wavy furrows, typically up to 100 m wide and 30 m deep, densely cover the shallowest, <400-m-deep portions of seafloor. Below this depth range, the seafloor exhibits coherent sets of evenly spaced, parallel, low-relief lineations (flutes) reaching 15+ km in length and extending in some areas to nearly 1000 m water depth. At their shallow termination, flutes are crosscut and obscured by chaotic iceberg scours. In several areas, the fluted seafloor pattern is complicated by nested sets of transverse, slightly sinuous or arcuate ridges that parallel bathymetric contours (Fig. 2 in Polyak et al., 2001). The combination of the above features allows their identification as glaciogenic (produced by grounded ice), being readily distinguishable from bedforms generated by other seabed-shaping agents such as currents or

slumps (e.g., Flood, 1983; Davies et al., 1997; Kuijpers et al., 2002). Flutes and transverse morainic ridges are characteristic of glaciated shelves, including the deep continental margin around Antarctica, where they are used as diagnostic features for identifying the former grounding of ice sheets (e.g., Davies et al., 1997; Polyak et al., 1997; Shipp et al., 1999; Ó Cofaigh et al., 2003). At these sites, flutes (or megascale lineations) are used as indicators of the orientation of ice movement. The transverse, isobath-parallel ridges likely mark the back stepping of ice grounding line with rising sea level during deglaciation. Iceberg scours, which have obliterated the shallower ridges and flutes at depths <350–400 m, reflect independent movement of many icebergs driven by winds and/or currents after the ice-shelf disintegration.

Subbottom sonar records show a clear picture of erosion of pre-glacial strata on the Chukchi Borderland (Fig. 2; see also Jakobsson et al., 2005) similar to that on glaciated shelves (e.g., Davies et al., 1997) and on the Lomonosov Ridge (Jakobsson, 1999; Polyak et al., 2001). Unstratified seismic units, identified elsewhere as glaciogenic diamictos, mostly occur as a thin veneer atop eroded surfaces but may form accumulations of several tens of meters thick where they fill erosional depressions or build morainic lobes.

The prevailing northwestern orientation of flutes in several areas of the Chukchi Borderland points to the NW sector of the Laurentide ice sheet as a major source for the flow of eroding ice (Fig. 1A) (Polyak et al., 2001; Jakobsson et al., 2005). Based on the comparison of subbottom sonar records from these areas and the Lomonosov Ridge, Jakobsson et al. (2005) tentatively

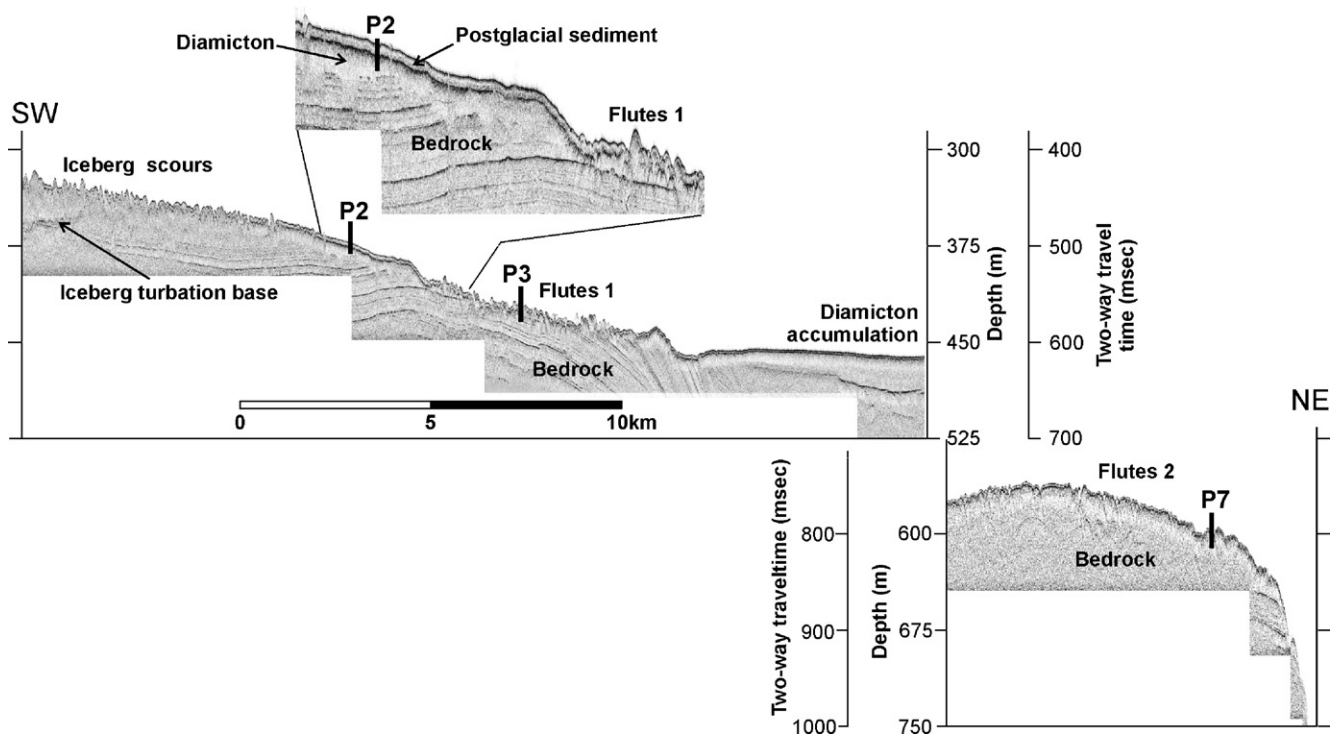


Figure 2. Subbottom chirp sonar records (HOTRAX-2005 data: Darby et al., 2005) across core sites P2/P3 and P7 (Fig. 1 for location). Blow-up fragment near P2 shows details of the upper strata. Data were collected with the USCGC Healy hull-mounted Knudsen 320 B/R chirp sonar system and post-processed using the software *Sioseis* (<http://sioseis.ucsd.edu>). Character of erosion (e.g., iceberg scouring vs. fluting) was verified using sidescan and swath bathymetry images.

proposed a similar age of this erosion, that is around OIS 6. To the southwest, flutes cover the Chukchi Margin with a different, nearly latitudinal orientation formed by west- or eastward ice flow (Figs. 1A–B) (Polyak et al., 2001). These bedforms do not extend to water depths >450 m, indicating a relatively thin eroding ice and its younger age in comparison with flutes located deeper—to >700 m in adjacent areas and to nearly 1000 m at some Northwind Ridge sites farther north. We will henceforth refer to the shallower (younger) and deeper (older) generations of flutes as 1 and 2, respectively.

Sediment-core records

Materials and methods

The US Geological Survey has collected a number of sediment cores from the Chukchi Borderland in 1992 (Cruise P1-92-AR) (Scientific Party, 1993). Cores were logged on the MST logger, X-rayed, described, and photographed after splitting (Phillips, R.L., personal communication, 2001); core P1 from the shelf edge has been analyzed in more detail with the focus on the Holocene environments (Darby et al., 2001; Darby and Bischof, 2004). Core sites at relatively shallow water depths on the ramp to the Northwind Ridge (Fig. 1B; Table 1) were characterized by geophysical seafloor data including SCICEX-1999 sidescan sonar and swath bathymetry mapping (Edwards and Coakley, 2003) and Healy-Oden Trans-Arctic Expedition (HOTRAX-2005) multibeam bathymetry and subbottom sonar profiling (Darby et al., 2005). As shown by these data, cores P2 to P7 are located within the eroded area that includes fluted fields 1 and 2 extending to depths of ~450 m and 750 m, respectively (Figs. 2 and 3; Polyak et al., 2001; Jakobsson et al., 2005). We focused our investigation on these cores to establish their stratigraphic correlation and to understand their relationship to ice-grounding processes. Sediment was analyzed for coarse grain size, composition of clasts >250 μm , and mineralogy of detrital iron-oxide grains in the 45–250 μm fraction matched to a circum-Arctic source database (Darby and Bischof, 1996; Darby, 2003). The combination of these approaches is especially efficient for determining sources of sediment delivered by icebergs and sea ice (e.g., Darby et al., 2002; Darby and Bischof, 2004). Also analyzed were benthic and planktonic foraminifers and stable-isotopes of planktonic foraminiferal tests. Age was determined by AMS ^{14}C dating of calcareous shells/tests where available (Table 2). Generated ^{14}C ages were calibrated using Marine04 curve in CALIB (Stuiver

and Reimer, 1993; version 5.0.2) with no regional correction (ΔR) applied because of large uncertainties with marine reservoir ages in Arctic waters, especially for deglaciation (Björck et al., 2003; Eiriksson et al., 2004). Resulting calibrated ages should be thus deemed as maximal; the actual ages during deglaciation could be younger by several hundred years. Difference in reservoir ages between benthic and planktonic material is expected to be negligible because of relatively shallow water depths at core sites and subsurface habitats of Arctic planktonic foraminifers (e.g., Volkman, 2000).

Results

All cores from the eroded sites end in compacted, gray diamict sediment except for P6, which is similar to P7 but stratigraphically shorter (Fig. 3). For comparison, none of the 40+ cores collected on the Chukchi Borderland outside the eroded areas as exemplified by core P9 contain similar sediments. Diamictons have a massive structure and a low, but consistent, coarse debris content (Fig. 4). Sediment is only moderately stiff, similar to diamictons under modern ice streams (Tulaczyk et al., 1998) and in troughs that were likely outlets for paleo-ice streams (e.g., Polyak et al., 1997; Dowdeswell et al., 2004). The lower portion of P1 is generally similar to diamictons in P2–P7 but somewhat softer and more enriched in randomly distributed coarse debris. Sediment recovered at the bottom of P3 has a composition mostly similar to the overlying diamicton but features well-preserved, partially lithified, fine burrow structures (Fig. 4).

The stratigraphies above the diamictons are different between cores from the two fluted fields, 1 and 2, corresponding to water depths above and below ~450 m. In the shallower area (cores P2 and P3) the stratigraphy includes <1-m-thick gray mud with variable, layered concentration of coarse clasts, topped with brownish to olive-gray, mostly fine-grained, soft mud (Figs. 3 and 4). The latter unit, which is readily correlated to cores from both deeper and shallower areas, increases in thickness towards the Chukchi shelf (e.g., core P1) along with a change from brown to olive-gray coloration. ^{14}C ages from P1 and P2 indicate that this top gray unit and a large portion of the gray clast-rich mud were deposited during and shortly before the Holocene, respectively (Figs. 3 and 4). A slight inversion in ages at 115–117 cm in P2 possibly resulted from redeposition such as by icebergs and does not significantly affect the results. We judge the age of 11,830 ^{14}C yr BP at 115 cm as too old as it gives an unrealistically old estimate for the bottom of Holocene sediment if used in constructing an age model. In cores P6 and P7 the post-diamict section is much thicker than in P2/P3 and includes another conspicuous brown mud unit at ~2-m level underlain by gray mud with fine, indistinct lamination (Fig. 3). Similar brown units are characteristic of interglacial/interstadial environments in the Northwind Ridge area and throughout the central Arctic Ocean (e.g., Phillips and Grantz, 1997; Jakobsson et al., 2000; Polyak et al., 2004), whereas laminated muds similar to those in P6/P7 have been described as turbidites (see also Campbell and Clark, 1977; Grantz et al., 1997). In core P6, two ages of ~40,000 ^{14}C yr BP, which may be infinite, were

Table 1
P1-92-AR (USGS) sediment cores on the ramp to Northwind Ridge

Core no.	Latitude N	Longitude W	Water depth (m)	Piston core length (cm)
P1	73° 42.4'	162° 44.6'	201	429
P2	73° 57.3'	161° 31.7'	369	348
P3	73° 59.7'	161° 23.2'	442	227
P6	74° 15.3'	160° 35.4'	580	570
P7	74° 30.4'	159° 57.9'	592	830
P9	74° 54.5'	158° 59.5'	1242	443

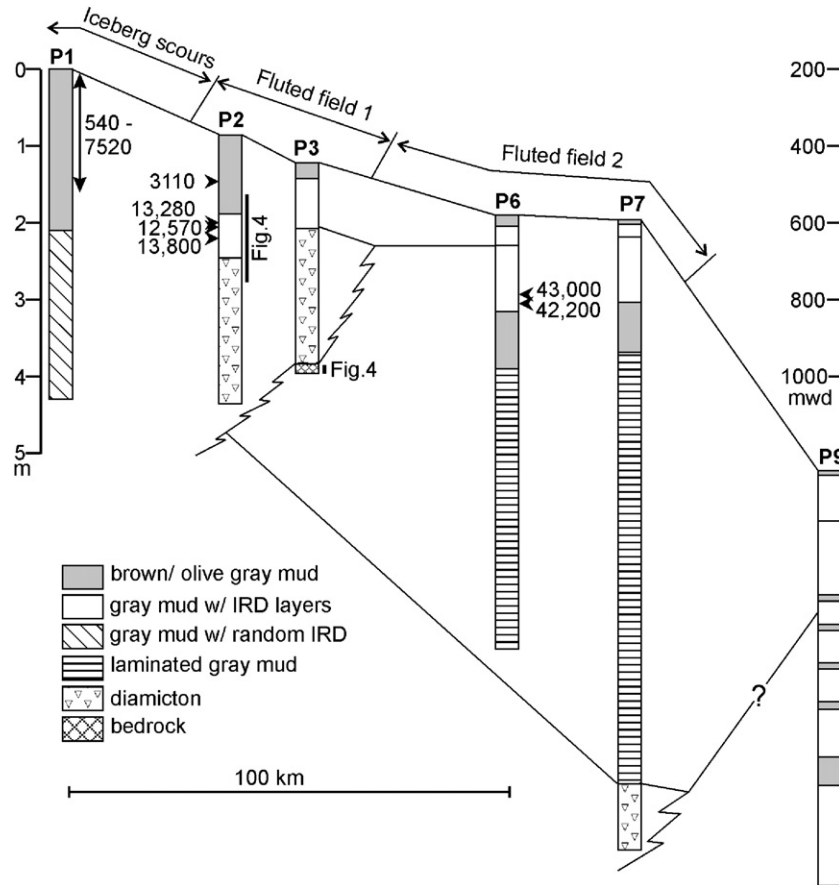


Figure 3. Simplified lithostratigraphy of sediment cores (Fig. 1 for location) with correlation lines shown for diamictons. Correlation with core P9 is based on the count of brown units (see also Phillips and Grantz, 1997). Scales for sediment (m) and water depth (mwd) are shown on the left and right, respectively. ^{14}C ages are shown next to cores P1/P2 (cal yr BP) and P6 (^{14}C yr BP). Portions of cores P2 and P3 used in Figure 4 are indicated by vertical bars.

obtained from the yellowish, foraminiferal-rich interval between 90 and 105 cm that may represent another interstadial. As no other interstadial-type units were identified above this interval, we tentatively date it as OIS 3 and the underlying brown unit as an older interglacial/interstadial.

The diamictons and underlying sediment contain only very sparse benthic foraminifers with poorly preserved and/or metamorphosed (brown) tests (Fig. 5A). Tentative identification indicates their affinity to taxa (*Lenticulina* sp., *Osangularia* ?

sp.) that are absent or very rare in Quaternary Arctic sediments, but are common for some Mesozoic and lower Cenozoic deposits from adjacent regions such as the North Sea basin (e.g., Jenkins and Murray, 1989). Foraminifers in post-diamict sediments contain common Quaternary Arctic assemblages dominated by planktonic *Neogloboquadrina pachyderma* (sinistral) and benthic *Cassidulina teretis*. Calcareous foraminifers occur mostly in low numbers and bear signs of dissolution, but form isolated abundance peaks such as around

Table 2
Accelerator mass spectrometer (AMS) ^{14}C dates^a

Lab no. ^b	Core no.	Depth in core (cm)	Material ^c	Reported age (^{14}C yr BP)	Calibrated age median and 2- σ range (cal yr BP) ^d
CAMS 88289	P2-T ^e	60–62	M	3270 \pm 35	3110 (2980–3230)
AMS 96605	P2	114–116	PF	11,830 \pm 70	13,280 (13,160–13,420)
AA55670	P2	116–117.5	PF	11,030 \pm 160	12,570 (12,080–12,890)
AA59201	P2	134–137.5	BF	12,340 \pm 90	13,800 (13,600–14,010)
AA42038	P6	92–93	PF	43,000 \pm 2300	N/A
AA42039	P6	104–105	PF	42,200 \pm 3000	N/A

^a Data for P1 have been reported earlier (Darby et al., 2001; Darby and Bischoff, 2004).

^b AA—Arizona AMS Facility, CAMS—Lawrence Livermore National Laboratory.

^c M—mollusk shell (*Thyasira* sp.), PF—planktonic foraminifers; BF—benthic foraminifers.

^d No ΔR applied.

^e P2-T–P2 trigger core.

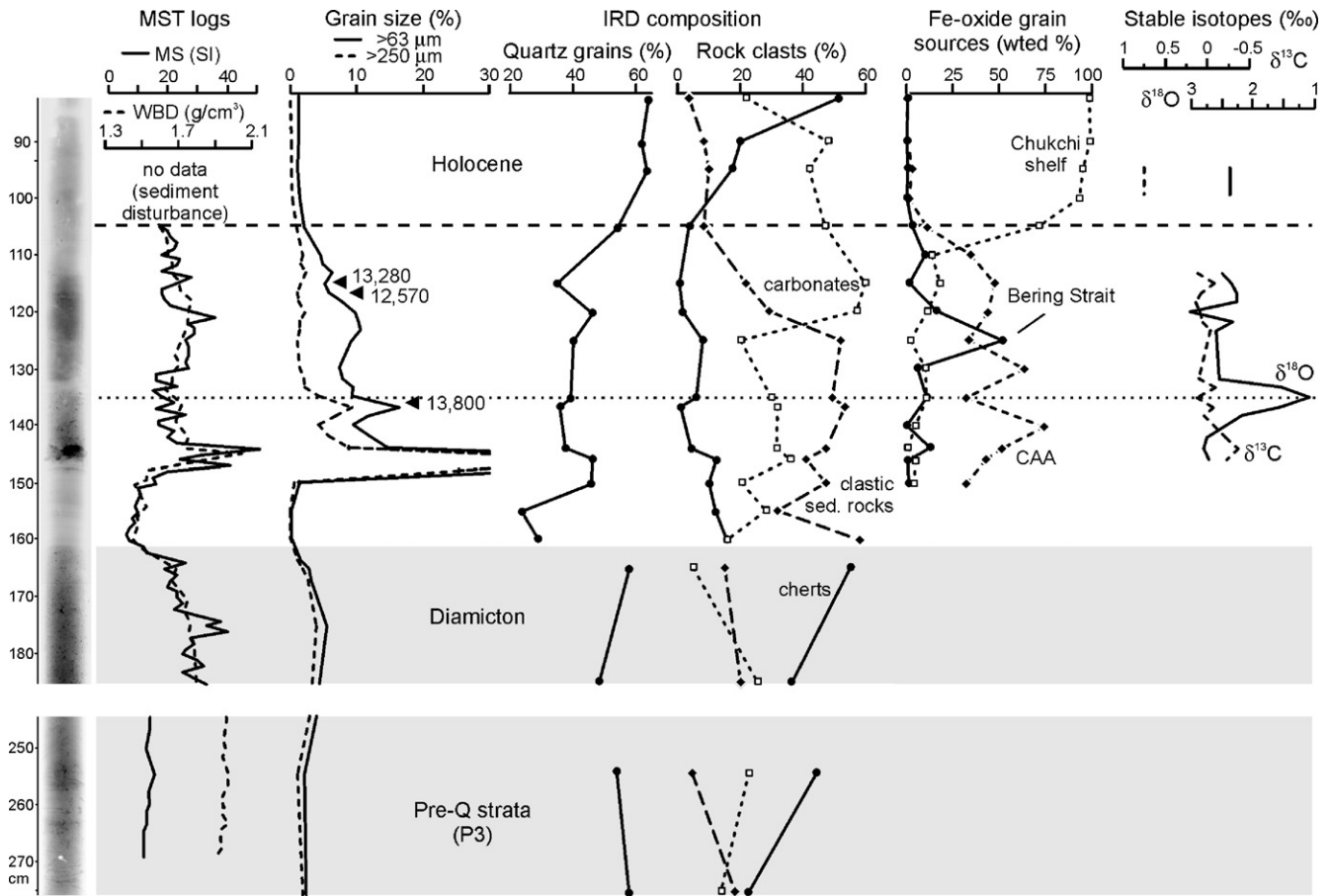


Figure 4. Sedimentary record from fluted field 1, composed of cores P2 (85–185 cm) and P3 (bedrock, 245–275 cm): X-ray image, MST logs (magnetic susceptibility and wet bulk density), sand grain size, IRD composition (mud-clump free), Fe-oxide grain source matches in postglacial sediment, and stable isotopes in *N. pachyderma* (sin). Ages (cal yr BP) are shown next to the sand curve. Stable-isotope data for the Holocene are spliced from the P2 trigger core (Fig. 6 for detail). Diamicton (P2) and pre-Quaternary sediment (P3) is highlighted; Holocene bottom and $\delta^{18}\text{O}$ minimum are marked by dashed and dotted lines, respectively.

115 and 135 cm in P2. In the Holocene, foraminifers are mostly represented by arenaceous species, which is common for many areas on the Arctic margins with bottom waters corrosive to CaCO_3 (e.g., Steinsund and Hald, 1994). The Holocene sediments also contain abundant dinocysts that are not found at other intervals in any of the studied cores (de Vernal, A., personal communication, 2003).

Stable-isotope measurements on *N. pachyderma* (sin) from P1 and P2 provide records for the last ~8000 and between

12,000 and 14,500 cal yr BP that complement the data from the Beaufort margin (Andrews and Dunhill, 2004) obtained for the time interval that remains uncharacterized in P1/P2 (Figs. 4, 6). The most prominent feature of the composite $\delta^{18}\text{O}$ record is a pronounced, almost 2‰ depletion event occurring on top of a prominent spike of coarse debris in P2, shortly after ca. 14,000 cal yr BP (uncorrected for ΔR). This, as well as a smaller $\delta^{18}\text{O}$ excursion ca. 1500 yr younger, coincide with calcareous foraminiferal abundance peaks. Taken

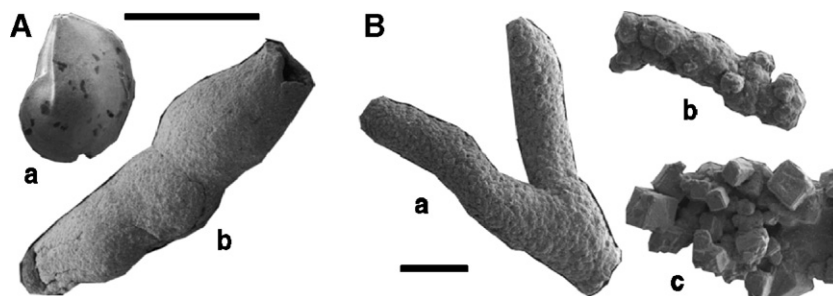


Figure 5. SEM images exemplifying bio- and chemogenic objects in bedrock and diamictons. Scale bars = 1 mm. (A) Calcareous benthic foraminifer *Lenticulina* sp. (a) and lithified, slightly pyritized burrow fill (b) from bedrock in P3. (B) Pyritized objects (biomorphs?) from diamicton in P7, featuring variable composition and morphology of pyrite grains. Specimen (c) with well-developed crystals has maximal content of Fe and S (24 and 19%, respectively).

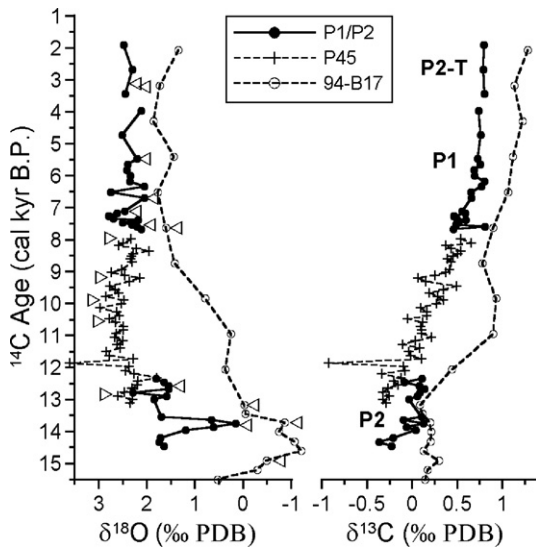


Figure 6. Correlation of stable-isotope records on the Chukchi margin (combined P1, P2, and P2-trigger cores: this paper and Darby et al., 2001), Beaufort margin (P45: Andrews and Dunhill, 2004), and the Mendeleev Ridge (94-B17: Poore et al., 1999). Age is interpolated between calibrated ^{14}C dates (no ΔR applied) shown by triangles next to $\delta^{18}\text{O}$ curves. The $\delta^{18}\text{O}$ values have been corrected for the effect of global sea-level rise (Fairbanks, 1990). P1/P2 and 94-B17 samples were analyzed at WHOI Paleo Mass Spectrometer Facility (www.whoi.edu/paleo/mass-spec), and P45 samples—at the University of Kiel.

together, the Chukchi/Beaufort stable-isotopic records show a pattern similar to those from the Mendeleev Ridge in the interior of the Amerasia Basin (Poore et al., 1999; Polyak et al., 2004), with mostly consistent offsets between the Mendeleev Ridge and Chukchi/Beaufort records that reflect a spatial stable-isotopic heterogeneity in the western Arctic Ocean and require further investigation (Fig. 6). The Mendeleev Ridge records are more likely to be affected by bioturbation than P1/P2 because of lower sedimentation rates; this may account for a sharper $\delta^{18}\text{O}$ depletion spike in P2.

Coarse debris in the diamictos as well as underlying bioturbated sediment recovered in P3 consists mostly (>95%) of yellowish-brown, hardened mud clumps shaped like pellets or burrow fills (Fig. 5). Also common are pyritized aggregations of various morphotypes (mostly cubic and globular) and chemical contents (concentrations of Fe and S measured by Energy Dispersive Spectroscopy on individual specimens vary between <10–25% and <5–20%, respectively). This composition of coarse fragments differs from the usual ice-rafted debris (IRD) in the Arctic Ocean but is similar to authigenic inclusions in various pre-Quaternary (Mesozoic to Cenozoic) strata from circum-Arctic regions (e.g., Yashin et al., 1985; Dixon et al., 1992). More sturdy mineral (mostly quartz) grains and rock clasts, which are more typical of the Arctic IRD (Darby and Bischof, 1996; Phillips and Grantz, 2001), are present in much lower numbers. Their content in the diamicton is variable and predominated by quartz grains, with cherts being most abundant among rock clasts (Fig. 4).

In the post-diamict sections, as well as in P1, the abundance of coarse debris is highly variable and it is composed almost entirely of quartz grains and rock clasts. The composition of

rock clasts between the diamicton and the Holocene unit in P2/P3 changes up-core from predominantly sedimentary rocks to carbonates, whereas Fe-oxide grain matches indicate mostly Canadian Arctic sources for finer grains throughout this interval. A notable exception is a spike in grains with Bering Strait affinity identified at 125 cm in P2 (Fig. 4) in conjunction with elevated contents of fine sand and coarse silt (45–125 μm size fractions). Holocene sediments have overall very low IRD abundances with a high percentage of quartz grains and cherts indicative of Alaskan sources (see also Darby et al., 2001), whereas predominant Fe-oxide grain type with a high content of altered magnetite has no known analog throughout the circum-Arctic margin and apparently originates from a local source on the Chukchi shelf (see also Darby and Bischof, 2004). This source may be from subsurface beds exposed near the shelf edge because similar magnetite grains are not common in surface sediments on the shelf to the south.

Interpretation

Ice-grounding events

The co-occurrence of diamictos in sediment cores with glaciogenic seafloor bedforms at the Chukchi margin strongly indicates that diamictos were formed subglacially, similar to numerous examples from glaciated continental margins in the Arctic and Antarctica (e.g., Davies et al., 1997; Polyak et al., 1997; Dowdeswell et al., 2004). This interpretation is consistent with the prominent erosional unconformity indicated by subbottom sonar records (Fig. 2). The sediment with burrow structures recovered beneath the diamicton in P3 apparently belongs to the folded and partially deformed pre-Quaternary bedrock (see also Phillips et al., 1988; Grantz et al., 1990). This inference is corroborated by the composition of coarse fragments and rare foraminifers found in diamictos and underlying sediments that bears similarity to various Mesozoic or lower Cenozoic deposits from the Arctic and subarctic margins (Jenkins and Murray, 1989; Dixon et al., 1992). Cretaceous strata outcrop under surficial sediments in many areas of the Chukchi shelf, but they appear to be overlain by progressively thickening Cenozoic deposits north- and eastwards (Phillips et al., 1988; Grantz et al., 1990). A more accurate determination of the bedrock age at the Chukchi margin is not yet attainable, and this age may differ between the cores from different water depths. The similarity in composition indicates that the diamictos were primarily formed from reworked local bedrock. Notably, preservation of unlithified and/or chemically unstable fragments, for example mud clumps and pyrite aggregations, is not common for redeposition in marine environments. In contrast, numerous bedrock fragments, including fragile pyrite clusters, are characteristic of glaciogenic diamictos that have assimilated frozen or pressurized sediment of the substratum such as in the Barents and Kara seas (Yashin et al., 1985; Polyak et al., 1997, 2000).

The lower portion of P1, which is also composed of mixed sediment, has high contents of coarse debris, predominantly quartz grains and rock clasts. The latter mostly consists of

erratic carbonates, similar to the uppermost pre-Holocene interval and unlike the diamictos in P2–P7 (Fig. 4). This difference can be explained by the iceberg-turbated nature of P1 pre-Holocene sediment, which is consistent with the evidence of intense iceberg scouring of the upper slope in both swath and subbottom sonar data (Fig. 2).

Different stratigraphic positions of the diamictos in cores P2/P3 and P7 (Fig. 3) indicate their different ages. A shorter post-diamict stratigraphy in P2/P3 agrees with the younger age of glacial erosion in fluted field 1, as inferred from its shallower bathymetric position. The missing section of a longer P6/P7 stratigraphy that includes at least one interglacial/interstadial lithological unit was apparently eroded in fluted field 1. The absence of interglacial/interstadial lithologies between the diamicton and the Holocene unit in P2/P3, the distribution of ^{14}C ages, and the position of $\delta^{18}\text{O}$ minimum in P2 (Figs. 4, 6) all indicate that the latest glacial event occurred during the LGM. This conclusion implies the advance of an extensive ice shelf or armada of tightly packed megabergs into the Amerasia Basin during the LGM, which is consistent with the absence of biogenic remains and extremely low sedimentation rates, possibly a hiatus throughout the basin between ca. 13,000 to 20,000 ^{14}C yr BP (Fig. 6 in Polyak et al., 2004). With a correction for the LGM sea level fall of ~ 120 m, the draft of ice grounded on the Chukchi margin was at least ~ 300 m, which implies its minimal overall thickness close to 350 m (with 1/8 to 1/10 of floating ice thickness above water).

The age of the diamicton recovered in P7 from fluted field 2 is less evident. Ages of $>40,000$ ^{14}C yr BP above the brown unit in P6 (Fig. 3) indicate that it is likely older than OIS 3. Samples examined from pre-Holocene sediments in P6/P7 including the brown unit are barren of dinocysts (de Vernal, A., personal communication, 2003), which are characteristic of full interglacial conditions of OIS 5e as demonstrated for the Eurasia basin of the Arctic Ocean (Matthiessen et al., 2001). This lack of dinocysts suggests that sediments recovered in P6/P7 are probably younger than OIS 5e. Based on these constraints we tentatively estimate the age of the diamicton in fluted field 2 as between OIS 4 to 5d. Unfortunately, the pre-LGM history of Laurentide glaciations in the Arctic is too poorly understood to be used for constraining the age of this erosion, but we note that the suggested time interval includes an inferred widespread intra-stage 5 glaciation in the Beringia region (Brigham-Grette et al., 2001).

While the ice that formed fluted field 2 is believed to have moved northwesterly, suggesting an origin to the southeast along the Laurentide northern margin (Polyak et al., 2001; Engels, 2004; Jakobsson et al., 2005), the direction of flutes in field 1 is unresolved. Polyak et al. (2001) suggested an East Siberian source for this ice mass, but geological studies in that area do not give grounds for reconstructions of a large LGM ice sheet (Gualtieri et al., 2003, 2005). Alternatively, the source could be the northwestern sector of the Laurentide ice sheet (Keewatin dome), which contained very large LGM ice volumes according to recent estimates (Tarasov and Peltier, 2004) and had natural passages for ice streaming via the large inter-island troughs of the Canadian Arctic Archipe-

lago (CAA) (Bischof and Darby, 1999a; Clark and Stokes, 2001; Stokes et al., 2005, 2006). We note that the trajectories of ice movement differ between the two generations of flutes, where field 2 indicates a deviation of Laurentide-originating ice masses from the straight course, as opposed to field 1. The cause of such pattern is unknown; one explanation implies the growth of an ice rise on the Chukchi Plateau that would obstruct the ice-shelf pathway. Alternatively, a Laurentide-sourced ice shelf may have been buttressed by ice masses that possibly invaded the central Arctic Ocean from other sources such as the Eurasian ice sheet during the formation of fluted field 2, but not at the LGM. This speculation is consistent with the finding of glaciogenic lineations along the Alaskan margin at water depths to ~ 700 m that align with flutes in field 2 (Fig. 1A; Engels, 2004). Glaciological modeling is needed to test the sources and configuration of ice shelves in the Arctic Ocean inferred from seafloor data.

Post-diamict stratigraphy and environments

Changes in sediment composition in post-diamict section in P2/P3 provide additional insight in late-glacial and postglacial environments. The marked difference in lithological composition between the diamictos and immediately overlying layers indicates different sources and also possibly a difference in subglacial vs. aquatic depositional environments, which would affect the redeposition of mud clumps and pyrite aggregates. The fine-grained interval immediately on top of the diamicton (150–160 cm; Fig. 4) may have formed under a yet cohesive, floating ice shelf, with an overlying prominent IRD spike marking the final break up. This event possibly relates to the youngest Laurentide-sourced IRD spike in the Fram Strait dated to ca. 16,000 cal yr BP (Darby et al., 2002), but the correlation needs to be tested by intermediately located sediment records from the central Arctic Ocean.

Compositions and high contents of IRD in late-glacial sediments in P2/P3, as well as in mixed sediment in P1, reflect predominant sedimentation from icebergs. A distinct shift from more numerous lithic clasts to carbonates at some time between ca. 12,000–13,000 cal yr BP (depending on marine reservoir ages) indicates a change in sediment source. It has been shown that detrital carbonates in the Arctic Ocean sediments are indicative of the source area in the northwestern part of the Canadian Arctic Archipelago (CAA), such as Banks and Victoria islands, from where IRD-dispersing icebergs drifted across the Canada basin onto the Chukchi margin and further into the interior of the Arctic Ocean (Bischof and Darby, 1997, 1999a; Phillips and Grantz, 2001). Multiple carbonate IRD events presumably related to this province have been documented in many sediment cores within and beyond the Canada Basin, including the late postglacial event potentially correlative to that in P2/P3 (Bischof and Darby, 1999b; Polyak et al., 2004). The preceding interval in P2/P3 is predominated by lithic clasts, mostly dark gray siltstones and shales similar to Meso-Cenozoic rocks occurring at the periphery of the Canada basin, notably in the Mackenzie area (e.g., Dixon et al., 1992; Darby and Bischof, 1996; Phillips and Grantz, 2001). A similar IRD composition,

generally rare for western Arctic Ocean cores, has been registered at the correlative stratigraphic level in other cores from the Chukchi area (Bischof and Darby, 1997, 2002). This composition probably reflects a diversion of carbonate-bearing CAA icebergs by a different drift pattern or their blockage by an ice barrier. We suggest that this pattern may be related to a more proximal source of the IRD assemblage than that of the carbonates, possibly from ice that decoupled from the outer margin of CAA or Mackenzie Trough, whereas carbonate-rich IRD marks deglaciation of CAA straits such as Amundsen Gulf and M'Clure Strait (Stokes et al., 2005, 2006). It is possible that the rise in sea level enhanced the export of icebergs from the latter sources.

The lithic-IRD enriched interval contains a prominent $\delta^{18}\text{O}$ minimum shortly after ca. 14,000 cal yr BP (Figs. 4, 6). Its very large magnitude, short duration, and location in deglacial sediment indicate that the $\delta^{18}\text{O}$ depletion was caused by a meltwater event (e.g., Jones and Keigwin, 1988; Stein et al., 1994; Spielhagen et al., 2005). The co-occurrence of this spike, as well as a smaller one ca. 1500 yr later, with foraminiferal abundance peaks probably reflects heightened sedimentation rates, and thus better preservation of calcite during meltwater discharge events. A correlative $\delta^{18}\text{O}$ minimum in the Mendeleev Ridge records has been interpreted to result from a meltwater pulse related to the retreat of the Laurentide ice sheet in the Mackenzie delta area (Poore et al., 1999; Hall and Chan, 2004; Polyak et al., 2004). Our identification of this event much closer to the Laurentide margin, and in association with numerous lithic clasts presumably originating from the Mackenzie area, provides further support to this interpretation. The alternative meltwater source from the more distant Eurasian margin, situated downstream in the prevailing surface circulation, is much less likely. The nearest known $\delta^{18}\text{O}$ depletion spike at the Laptev Sea margin is ca. 1000 yr younger and probably has a source different from the Amerasia Basin event (Spielhagen et al., 2005).

Both geological data and geodetic modeling indicate that very large volumes of ice and/or meltwater discharged into the Arctic Ocean at the northwestern Laurentide margin between ca. 13,000 and 11,000 cal yr BP (Lemmen et al., 1994; Tarasov and Peltier, 2005, 2006). The largest pulse, possibly associated with the flooding from Lake Agassiz, has been computed to occur shortly after 13,000 cal yr BP (Tarasov and Peltier, 2005, 2006). The reported $\delta^{18}\text{O}$ minimum in the Amerasia Basin appears to be ca. 1000 yr older (Fig. 6), but its accurate dating is hindered by the uncertainty in Arctic marine reservoir ages that may be considerably larger than the global average (Eiriksson et al., 2004). Furthermore, especially large reservoir ages of around 1000 yr are expected in the northern polar areas for the last deglaciation (Björck et al., 2003). With such correction, the timing of the Amerasia Basin $\delta^{18}\text{O}$ depletion spike would closely match the modeled peak of Laurentide discharge that was proposed as a possible trigger for the Younger Dryas climatic oscillation (Tarasov and Peltier, 2005, 2006). We note that this $\delta^{18}\text{O}$ spike has a much larger magnitude than the ca. 1500-yr younger $\delta^{18}\text{O}$ excursion that occurs both at

the Chukchi and Beaufort margin (Fig. 6) and has been correlated to the latest and best documented pulse of Lake Agassiz drainage into the Arctic Ocean shortly before 11,000 cal yr BP (Fisher et al., 2002; Andrews and Dunhill, 2004). This pattern of $\delta^{18}\text{O}$ records in the Amerasia Basin indicates the profound significance of the Laurentide meltwater discharge at the onset of Younger Dryas, although its exact mechanisms such as the contribution of outflow vs. icebergs remain elusive (Lowell et al., 2005; Tarasov and Peltier, 2006). This discussion underscores the importance of refining the deglacial chronology at the northwestern Laurentide margin and the chronostratigraphy of sediment cores in the Arctic Ocean. This task is especially important in view of the ongoing discussion on the forcings of the Younger Dryas cooling, a favorite paleoclimatic example of abrupt climatic change (Broecker, 2003; Lowell et al., 2005; Tarasov and Peltier, 2005; Jennings et al., 2006).

The spike in Fe-oxide grains sourced to the Bering Strait (Fig. 4) is estimated to occur between ca. 12,000–13,000 cal yr BP, closely matching the timing of the initial inundation of the strait (Elias et al., 1996). This depositional event is not reflected in the coarse-clast record, but it is characterized by elevated contents of coarse silt to fine sand grains, which indicates that it is probably related to redeposition of winnowed sediment resulting from the initiation of the Bering water inflow into the Arctic Ocean.

The composition of mostly fine-grained Holocene sediment with elevated IRD contents of quartz grains and cherts as well as Chukchi shelf Fe-oxide sources (see also Darby et al., 2001; Darby and Bischof, 2004) suggests the significance of sea-ice rafting from southerly and southeastern (Alaskan) areas and possibly cross-shelf/downslope sediment load transport. Interestingly, both the recovered bedrock and diamictons also have a similar IRD composition (mud-clump free). This indicates the common provenance for preglacial and interglacial (Holocene) sedimentation. It is also possible that a portion of Holocene sediment is redeposited from bedrock outcrops on the Chukchi shelf (Phillips et al., 1988).

Conclusions

Sediment-core data from the Chukchi margin (ramp to the Northwind Ridge) confirm the existence of two generations of glacial erosion as inferred earlier from seafloor geophysical records (Polyak et al., 2001). Sediment stratigraphies from the two fluted fields extending to water depths of ~450 m and 750 m contain heterochronous glaciogenic diamictons that unconformably overlie Mesozoic or Cenozoic substrata. The diamictons resemble subglacial deposits found elsewhere, and they are distinctly different from overlying sediments deposited in iceberg-dominated environments as well as from iceberg-turbated sediments at shallower water depths, indicating that the most likely agents of erosion were ice sheets or shelves. We conclude that the erosion and emplacement of diamicton in the shallower field 1 occurred during the LGM, whereas the age of erosion at greater water depths is tentatively placed between OIS 4 and 5d.

More conclusive age determination of this major glacial event is important for clarification of its Arctic-wide context. Orientation of flutes in the two fields differs substantially, being near latitudinal in field 1 and northwesterly in the older field 2. We believe that both erosional events were caused by ice masses originating from the northwestern margin of the Laurentide ice sheet and the divergent trajectories possibly reflect different glaciological settings, with more ice intruding the Arctic Ocean during the earlier event. The presence of several-hundred-meter-thick ice extending from the CAA across the Canada Basin is a significant feature to be considered in paleoglaciological and paleoclimatic models. Arctic ice shelves might provide an explanation for at least a portion of an apparent discrepancy between the sea-level and marine oxygen-isotope record, equivalent to ~20 m of sea level, during the LGM (Clark and Mix, 2002) and potentially larger discrepancies during some of the earlier glaciations.

The early post-glacial sedimentation on the Chukchi margin was controlled by iceberg rafting from variable sources. Carbonate-rich CAA sources that typically characterize IRD spikes in Amerasia Basin were not fully represented until some time after ca. 13,000 cal yr BP, being possibly blocked from the Chukchi margin by ice from more proximal sources at the fringes of CAA and Mackenzie area and/or limited by low sea levels. This time interval encompasses a meltwater event indicated by a pronounced oxygen-isotope depletion spike that has also been observed on the Mendeleev Ridge, almost 1000 km away. The presence of this spike in the Chukchi sediments corroborates the earlier interpretation that the origin of meltwater was probably related to deglaciation in the Mackenzie delta area. If corrected for a ~1000-yr deglacial reservoir age (Björck et al., 2003), this $\delta^{18}\text{O}$ minimum approximates the modeled peak of Laurentide meltwater discharge into the Arctic Ocean at ca. 13,000 cal yr BP that was hypothesized to have triggered the Younger Dryas cooling (Tarasov and Peltier, 2005, 2006). A subsequent pulse of coarse silt to fine sand sedimentation with the Bering Strait source probably marks the initial inundation of the strait and the inflow of Pacific water into the Arctic Ocean. The Holocene sedimentation on the Chukchi margin was controlled by marine processes and sea ice rather than iceberg rafting, which highlights a profound difference between glacial and interglacial environments in the Arctic Ocean.

Acknowledgments

Work on this paper was supported by the USA National Science Foundation awards OPP-0136238 and 0136171 to Polyak and Darby. R.L. Phillips (USGS) kindly provided us with the core material, original core logs, and X-rays. D. Ostermann (WHOI) directed stable-isotope analyses. A. de Vernal (GEOTOP-UQAM) analyzed a series of samples for dinocysts. S. Bhattacharya (OSU) helped with SEM/EDS imaging/analysis. Reviews by J.B. Anderson and A. Kuijpers helped to improve the manuscript. This is Byrd Polar Research Center Contribution No. C-1343.

References

- Andrews, J.T., Dunhill, G., 2004. Early to mid-Holocene Atlantic water influx and deglacial meltwater events, Beaufort Sea slope, Arctic Ocean. *Quaternary Research* 61, 14–21.
- Bischof, J.F., Darby, D.A., 1997. Mid- to Late Pleistocene ice drift in the western Arctic Ocean: evidence for a different circulation in the past. *Science* 277, 74–78.
- Bischof, J.F., Darby, D.A., 1999a. Quaternary ice transport in the Canadian Arctic and extent of Late Wisconsinan glaciation in the Queen Elizabeth Islands. *Canadian Journal of Earth Sciences* 36, 2007–2022.
- Bischof, J.F., Darby, D.A., 1999b. Sequence of Laurentide ice decay recognized in Late Pleistocene to Holocene sediments of the western Arctic Ocean. *Eos, Transactions AGU* 80 (46) (Fall Meeting Supplement, F534).
- Bischof, J.F., Darby, D.A., 2002. A thick, grounded ice shelf in the Northwind Ridge region, western Arctic Ocean? *Eos, Transactions AGU* 83 (47) (Fall Meeting Supplement, F782).
- Björck, S., Koc, N., Skog, G., 2003. Consistently large marine reservoir ages in the Norwegian Sea during the last Deglaciation. *Quaternary Science Reviews* 22, 429–435.
- Blasco, S.M., Fortin, G., Hill, P.R., O'Connor, M.J., Brigham-Grette, J., 1990. The late Neogene and Quaternary stratigraphy of the Canadian Beaufort continental shelf. In: Grantz, A., Johnson, L., Sweeney, J.F. (Eds.), *The Geology of North America, Vol. L. The Arctic Ocean region*. Geol. Soc. Amer., Boulder, pp. 491–502.
- Brigham-Grette, J., Hopkins, D.M., Ivanov, V.F., Basilyan, A.E., Benson, S.L., Heiser, P.A., Pushkar, V.S., 2001. Last Interglacial (isotope stage 5) glacial and sea-level history of coastal Chukotka Peninsula and St. Lawrence Island, Western Beringia. *Quaternary Science Reviews* 20, 419–436.
- Broecker, W.S., 2003. Does the trigger for abrupt climate change reside in the ocean or in the atmosphere? *Science* 300, 1519–1522.
- Bromwich, D.H., Toracinta, E.R., Wei, H., Oglesby, R.J., Fastook, J.L., Hughes, T.J., 2004. Polar MM5 simulations of the winter climate of the Laurentide Ice Sheet at the LGM. *Journal of Climate* 17, 3415–3433.
- Budd, W.F., Coustts, B., Warner, R.C., 1998. Modeling the Antarctic and Northern Hemisphere ice-sheet changes with global climate through the glacial cycle. *Annals of Glaciology* 27, 153–160.
- Campbell, J.S., Clark, D.L., 1977. Pleistocene turbidites of the Canada Abyssal Plain of the Arctic Ocean. *Journal of Sedimentary Petrology* 47, 657–670.
- Clark, P.U., Mix, A.C., 2002. Ice sheets and sea level of the Last Glacial Maximum. *Quaternary Science Reviews* 21, 1–7.
- Clark, C.D., Stokes, C.R., 2001. Extent and basal characteristics of the M'Clintock Channel ice stream. *Quaternary International* 86, 81–101.
- Darby, D.A., 2003. Sources of sediment found in sea ice from the western Arctic Ocean, new insights into processes of entrainment and drift patterns. *Journal of Geophysical Research* 108 (C8), 3257, doi:10.1029/2002JC001350, 13-1–13-10.
- Darby, D.A., Bischof, J.F., 1996. A statistical approach to source determination of lithic and Fe-oxide grains: an example from the Alpha Ridge, Arctic Ocean. *Journal of Sedimentary Research* 66, 599–607.
- Darby, D.A., Bischof, J.F., 2004. A Holocene record of changing Arctic Ocean ice drift analogous to the effects of Arctic Oscillation. *Paleoceanography* 19, PA1027 (9 pp).
- Darby, D.A., Bischof, J.F., Cutter, G., deVernal, A., Hillaire-Marcel, C., Dwyer, G., McManus, J., Osterman, L., Polyak, L., Poore, R.Z., 2001. New record of pronounced changes in Arctic Ocean circulation and climate. *Eos* 82 (49), 603–607.
- Darby, D.A., Bischof, J.F., Spielhagen, R.F., Marshall, S.A., Herman, S.W., 2002. Arctic ice export events and their potential impact on global climate during the late Pleistocene. *Paleoceanography* 17 (2), 15-1–15-17.
- Darby, D.A., Jakobsson, M., Polyak, L., 2005. Icebreaker expedition collects key Arctic seafloor and ice data. *Eos* 86 (52), p. 549, 552.
- Davies, T.A., Bell, T., Cooper, A.K., Josenhans, H., Polyak, L., Solheim, A., Stoker, M.S., Stravers, J.A. (Eds.), 1997. *Glaciated Continental Margins: An Atlas of Acoustic Images*. Chapman and Hall, London. 315 pp.
- Dixon, J., Dietrich, J.R., McNeil, D.H., 1992. Upper Cretaceous to Pleistocene sequence stratigraphy of the Beaufort-Mackenzie and Banks

- Island areas, northwest Canada. Geological Survey of Canada Bulletin 407 (90 pp).
- Dowdeswell, J.A., Ó Cofaigh, C., Pudsey, C.J., 2004. Thickness and extent of the subglacial till layer beneath an Antarctic paleo-ice stream. *Geology* 32, 13–16.
- Dyke, A.S., Andrews, J.T., Clark, P.U., England, J.H., Miller, G.H., Shaw, J., Veillette, J.J., 2002. The Laurentide and Innuitian ice sheets during the Last Glacial Maximum. *Quaternary Science Reviews* 21, 9–31.
- Edwards, M., Coakley, B., 2003. SCICEX investigations of the Arctic Ocean System. *Chemie der Erde* 63, 281–328.
- Eiriksson, J., Larsen, G., Knudsen, K.L., Heinemeier, J., Simonarson, L.A., 2004. Marine reservoir age variability and water mass distribution in the Iceland Sea. *Quaternary Science Reviews* 23, 2247–2268.
- Elias, S.A., Short, S.K., Nelson, C.H., Birks, H.H., 1996. Life and times of the Bering land bridge. *Nature* 382, 60–63.
- Engels, J.L., 2004. New evidence for ice shelf flow across the Alaska and Beaufort margins, Arctic Ocean. PhD thesis, University of Hawaii.
- Fairbanks, R.G., 1990. The age and origin of the “Younger Dryas climate event” in Greenland ice cores. *Paleoceanography* 5, 937–948.
- Fisher, T.G., Smith, D.G., Andrews, J.T., 2002. Preboreal oscillation caused by a glacial Lake Agassiz flood. *Quaternary Science Reviews* 21, 873–878.
- Flood, R.D., 1983. Classification of sedimentary furrows and a model for furrow initiation and evolution. *Geological Society of America Bulletin* 94, 630–639.
- Grantz, A., May, S.D., Hart, P.E., 1990. Geology of the Arctic continental margin of Alaska. In: Grantz, A., Johnson, L., Sweeney, J.F. (Eds.), *The geology of North America, Vol. L. The Arctic Ocean region*. Geological Society of America, Boulder, pp. 257–288.
- Grantz, A., Phillips, R.L., Mullen, M.W., Starratt, S.W., Jones, G.A., Naidu, A.S., Finney, B.P., 1997. Character, paleoenvironment, rate of accumulation, and evidence for seismic triggering of Holocene turbidites, Canada Abyssal Plain, Arctic Ocean. *Marine Geology* 133, 51–73.
- Grosswald, M.G., Hughes, T.J., 1999. The case for an ice shelf in the Pleistocene Arctic Ocean. *Polar Geography* 23, 23–54.
- Gualtieri, L., Vartanyan, S., Brigham-Grette, J., Anderson, P.M., 2003. Pleistocene raised marine deposits on Wrangel Island, northeast Siberia and implications for the presence of an East Siberian ice sheet. *Quaternary Research* 59, 399–410.
- Gualtieri, L., Vartanyan, S.L., Brigham-Grette, J., Anderson, P.M., 2005. Evidence for an ice-free Wrangel Island, northeast Siberia during the Last Glacial Maximum. *Boreas* 34, 264–273.
- Hall, J.M., Chan, L.-H., 2004. Ba/Ca in *Neoglobobadrina pachyderma* as an indicator of deglacial meltwater into the western Arctic Ocean. *Paleoceanography* 19, PA1017 (9 pp).
- Hughes, T.J., Denton, G.H., Grosswald, M.G., 1977. Was there a late Wurm ice sheet? *Nature* 266, 596–602.
- Hunkins, K.L., Herron, T., Kutschale, H.W., Peter, G., 1962. Geophysical studies of the Chukchi Cap, Arctic Ocean. *Journal of Geophysical Research* 67, 235–247.
- Jakobsson, M., 1999. First high-resolution chirp sonar profiles from the central Arctic Ocean reveal erosion of Lomonosov Ridge sediments. *Marine Geology* 158, 111–123.
- Jakobsson, M., Lovlie, R., Al-Hanbali, H., Arnold, E., Backman, J., Morth, M., 2000. Manganese and color cycles in Arctic Ocean sediments constrain Pleistocene chronology. *Geology* 28, 23–26.
- Jakobsson, M., Lovlie, R., Arnold, E.M., Backman, J., Polyak, L., Knutsen, J.-O., Musatov, E., 2001. Pleistocene stratigraphy and paleoenvironmental variation from Lomonosov Ridge sediments, central Arctic Ocean. *Global and Planetary Change* 31, 1–22.
- Jakobsson, M., Gardner, J.V., Vogt, P., Mayer, L.A., Armstrong, A., Backman, J., Brennan, R., Calder, B., Hall, J.K., Kraft, B., 2005. Multibeam bathymetric and sediment profiler evidence for ice grounding on the Chukchi Borderland, Arctic Ocean. *Quaternary Research* 63, 150–160.
- Jenkins, D.G., Murray, J.W. (Eds.), 1989. *Stratigraphical Atlas of Fossil Foraminifera*, 2nd ed. Ellis Horwood, Chichester. 593 pp.
- Jennings, A.E., Hald, M., Smith, M., Andrews, J.T., 2006. Freshwater forcing from the Greenland Ice Sheet during the Younger Dryas: evidence from southeastern Greenland shelf cores. *Quaternary Science Reviews* 25, 282–298.
- Jones, G.A., Keigwin, L.D., 1988. Evidence from Fram Strait (78°N) for early deglaciation. *Nature* 336, 56–59.
- Kristoffersen, Y., Coakley, B., Jokat, W., Edwards, M., Brekke, H., Gjengedal, J., 2004. Seabed erosion on the Lomonosov Ridge, central Arctic Ocean: a tale of deep draft icebergs in the Eurasia Basin and the influence of Atlantic water inflow on iceberg motion? *Paleoceanography* 19, PA3006 (14 pp).
- Kuijpers, A., Hansen, B., Huhnerbach, V., Larsen, B., Nielsen, T., Werner, F., 2002. Norwegian Sea overflow through the Faroe–Shetland gateway as documented by its bedforms. *Marine Geology* 188, 147–164.
- Lemmen, D.S., Duk-Rodkin, A., Bednarski, J.M., 1994. Late glacial drainage systems along the northwestern margin of the Laurentide Ice Sheet. *Quaternary Science Reviews* 13, 805–828.
- Lowell, T.V., Fisher, T.G., Comer, G.C., Hajdas, I., Waterson, N., Glover, K., Loope, H.M., Schaefer, J.M., Rinterknecht, V., Broecker, W., Denton, G., Teller, J.T., 2005. Testing the Lake Agassiz meltwater trigger for the Younger Dryas. *Eos* 86, p. 365, 372.
- Matthiessen, J., Knies, J., Nowaczyk, N.R., Stein, R., 2001. Late Quaternary dinoflagellate cyst stratigraphy at the Eurasian continental margin, Arctic Ocean: indications for Atlantic water inflow in the past 150,000 years. *Global and Planetary Change* 31, 65–86.
- Mercer, J.H., 1970. A former ice sheet in the Arctic Ocean. *Palaeogeography, Palaeoclimatology, Palaeoecology* 8, 19–27.
- Ó Cofaigh, C., Pudsey, C.J., Dowdeswell, J.A., Morris, P., 2003. Evolution of subglacial bedforms along a paleo-ice stream, Antarctic Peninsula continental shelf. *Geophysical Research Letters* 29, 41-1–41-4.
- Phillips, R.L., Grantz, A., 1997. Quaternary history of sea ice and paleoclimate in the Amerasia basin, Arctic Ocean, as recorded in the cyclical strata or Northwind Ridge. *Geological Society of America Bulletin* 109, 1101–1115.
- Phillips, R.L., Grantz, A., 2001. Regional variations in provenance and abundance of ice-rafted clasts in Arctic Ocean sediments: implications for the configuration of late Quaternary oceanic and atmospheric circulation in the Arctic. *Marine Geology* 172, 91–115.
- Phillips, R.L., Pickthorn, L.G., Rearic, D.M., 1988. Late Cretaceous sediments from the northeast Chukchi Sea. *US Geological Survey Circular* 1016, 187–189.
- Polyak, L., Forman, S.L., Herlihy, F.A., Ivanov, G., Krinitsky, P., 1997. Late Weichselian deglacial history of the Svyataya (Saint) Anna Trough, northern Kara Sea, Arctic Russia. *Marine Geology* 143, 169–188.
- Polyak, L., Levitan, M., Gataullin, V., Khusid, T., Mikhailov, V., Mukhina, V., 2000. The impact of glaciation, river-discharge, and sea-level change on Late Quaternary environments in the southwestern Kara Sea. *International Journal of Earth Sciences* 89, 550–562.
- Polyak, L., Edwards, M.H., Coakley, B.J., Jakobsson, M., 2001. Ice shelves in the Pleistocene Arctic Ocean inferred from glaciogenic deep-sea bedforms. *Nature* 410 (6827), 453–457.
- Polyak, L., Curry, W.B., Darby, D.A., Bischof, J., Cronin, T.M., 2004. Contrasting glacial/interglacial regimes in the western Arctic Ocean as exemplified by a sedimentary record from the Mendeleev Ridge. *Palaeogeography, Palaeoclimatology, Palaeoecology* 203, 73–93.
- Poore, R.Z., Osterman, L., Curry, W.B., Phillips, R.L., 1999. Late Pleistocene and Holocene meltwater events in the western Arctic Ocean. *Geology* 27, 759–762.
- Scientific Party, 1993. Cruise to the Chukchi Borderland, Arctic Ocean. *Eos* 74, 253–254.
- Shipp, S., Anderson, J., Domack, E., 1999. Late pleistocene-holocene retreat of the West Antarctic ice-sheet system in the Ross Sea: part 1—Geophysical results. *Geological Society of America Bulletin* 111, 1486–1516.
- Siegert, M.J., Marsiat, I., 2001. Numerical reconstructions of LGM climate across the Eurasian High Arctic. *Quaternary Science Reviews* 20, 1595–1605.
- Spielhagen, R.F., Erlenkeuser, H., Siegert, C., 2005. History of freshwater runoff across the Laptev Sea (Arctic) during the last deglaciation. *Global and Planetary Change* 48, 187–207.
- Stein, R., Nam, S.-I., Schubert, C., Vogt, C., Fütterer, D., Heinemeier, J., 1994. The last deglaciation event in the eastern central Arctic Ocean. *Science* 264, 692–696.
- Steinsund, P.I., Hald, M., 1994. Recent calcium carbonate dissolution in the

- Barents Sea: paleoceanographic applications. *Marine Geology* 117, 303–316.
- Stokes, C.R., Clark, C.D., Darby, D.A., Hodgson, D.A., 2005. Late Pleistocene ice export events into the Arctic Ocean from the M'Clure Strait Ice Stream, Canadian Arctic Archipelago. *Global and Planetary Change* 49, 139–162.
- Stokes, C.R., Clark, C.D., Winsborrow, M.C.M., 2006. Subglacial bedform evidence for a major palaeo-ice stream in Amundsen Gulf and its retreat phases, Canadian Arctic Archipelago. *Journal of Quaternary Science* 21, 399–412.
- Stuiver, M., Reimer, P.J., 1993. Extended 14-C database and revised CALIB 3.0 14-C age calibration program. *Radiocarbon* 35, 215–230.
- Svendsen, J.I., Alexanderson, H., Astakhov, V.I., Demidov, I., Dowdeswell, J.A., Funder, S., Gataullin, V., Henriksena, M., Hjort, C., Houmark-Nielsen, M., Hubberten, H.W., Olfsson, I., Jakobsson, M., Kjær, K.H., Larsen, E., Lokrantz, H., Pekka Lunkka, J., Lyså, A., Mangerud, J., Matiouchkov, A., Murray, A., Möller, P., Niessen, F., Nikolskaya, O., Polyak, L., Saarnisto, M., Siegert, M., Spielhagen, R.F., Stein, R., 2004. Late Quaternary ice sheet history of northern Eurasia. *Quaternary Science Reviews* 23, 1229–1271.
- Tarasov, L., Peltier, W.R., 2004. A geophysically constrained large ensemble analysis of the deglacial history of the North American ice sheet complex. *Quaternary Science Reviews* 23, 359–388.
- Tarasov, L., Peltier, W.R., 2005. Arctic freshwater forcing of the Younger Dryas cold reversal. *Nature* 435, 662–665.
- Tarasov, L., Peltier, W.R., 2006. A calibrated deglacial drainage chronology for the North American continent: evidence of an Arctic trigger for the Younger Dryas. *Quaternary Science Reviews* 25, 659–688.
- Tulaczyk, S., Kamb, B., Scherer, R.P., Engelhardt, H.F., 1998. Sedimentary processes at the base of a West Antarctic ice stream: constraints from textural and compositional properties of subglacial debris. *Journal of Sedimentary Research* 68, 487–496.
- Vogt, P.R., Crane, K., Sundvor, E., 1994. Deep Pleistocene iceberg plowmarks on the Yermak Plateau: sidescan and 3.5 kHz evidence for thick calving ice fronts and a possible marine ice sheet in the Arctic Ocean. *Geology* 22, 403–406.
- Volkman, R., 2000. Planktic foraminifers in the outer Laptev Sea and the Fram Strait—Modern distribution and ecology. *Journal of Foraminiferal Research* 30, 157–176.
- Yashin, D.S., Mel'nitsky, V.Ye., Kirillov, O.V., 1985. Structure and composition of bottom deposits of the Barents Sea. In: Verba, M.L. (Ed.), *Geologicheskoe stroenie Barentsevo-Karskogo shel'fa* (Geological structure of the Barents and Kara Sea shelf). *Sevmorgeologia*, Leningrad, pp. 101–115 (in Russian).